

Extracting GHZ states from linear cluster states

J. de Jong¹, F. Hahn^{1,2}, N. Tcholtchev³, M. Hauswirth^{1,3}, and A. Pappa^{1,3}

¹ *Electrical Engineering and Computer Science Department,
Technische Universität Berlin, 10587 Berlin, Germany*

² *Dahlem Center for Complex Quantum Systems, Freie Universität Berlin, 14195 Berlin, Germany and*

³ *Fraunhofer Institute for Open Communication Systems - FOKUS, 10589 Berlin, Germany*

(Dated: May 16, 2023)

Quantum information processing architectures typically only allow for nearest-neighbour entanglement creation. In many cases, this prevents the direct generation of GHZ states, which are commonly used for many communication and computation tasks. Here, we show how to obtain GHZ states between nodes in a network that are connected in a straight line, naturally allowing them to initially share linear cluster states. We prove a strict upper bound of $\lfloor (n+3)/2 \rfloor$ on the size of the set of nodes sharing a GHZ state that can be obtained from a linear cluster state of n qubits, using local Clifford unitaries, local Pauli measurements, and classical communication. Furthermore, we completely characterize all selections of nodes below this threshold that can share a GHZ state obtained within this setting. Finally, we demonstrate these transformations on the IBMQ Montreal quantum device for linear cluster states of up to $n = 19$ qubits.

I. INTRODUCTION

Recent years have seen exciting developments in quantum computation and communication, both in theory and experiment. Building upon the year-long research on bipartite settings, focus has now also turned towards multipartite settings, where multiple vertices in a network share quantum resources between them. While the correlations of Greenberger-Horne-Zeilinger (GHZ) states [1] have naturally been the first to explore, other types of graph states [2] have also been extensively examined [3–6]. The possible transformations between quantum states is a topic that is heavily studied [7–11], and while several hardness results have emerged [12, 13], a lot of practical questions remain unanswered.

But why should we be interested in transforming one quantum state to another in the first place? One reason can be that it is not always possible to create the exact state that is necessary to perform a specific task, and we need to ‘retrieve’ it from some other state that is more practical to build. For example, while the underlying network architecture might allow for nearest-neighbour interactions, it might not allow for the direct distribution of large GHZ states between distant parties. Here we show that there is an indirect remedy for this deficiency using suitable transformations of the distributed quantum states. We focus on the transformation of *linear cluster states* [7], that arise naturally in linear networks. In particular we investigate the transformation to GHZ states, which are widely used in many quantum communication tasks including *anonymous transmission* [14], *secret sharing* [15, 16] and *(anonymous) conference key agreement* [17–19].

Such transformations require the removal of some of the qubits from the state by measuring them, such that only a selected subset of the qubits of the resource linear cluster state can in the end belong to the target GHZ state. We refer to these transformations as *GHZ extractions*. A previous study [20] showed how to extract three- and four-partite GHZ states from linear cluster states. Moreover, other works [21, 22] study a specific selection of the qubits of an odd-partite resource state. Here, we conclude this study by providing a complete characterisation of which GHZ extractions are pos-

sible and which are not. Very importantly, we provide a tight upper bound to the size of the largest GHZ state that can be extracted, equal to $\lfloor (n+3)/2 \rfloor$; interestingly this is slightly higher than the bound of $n/2$ conjectured in Ref. [7] and than the sizes of the states extracted in the aforementioned studies [21, 22]. In addition to our theoretical analysis, we perform demonstrations of implementations of the GHZ extractions from linear cluster states with $n \in \{5, 7, \dots, 19\}$ qubits on the IBMQ Montreal device.

Our manuscript is organized as follows: The notation, technical terminology and main definitions are introduced in Section II. Section III contains the main theoretical results. In Section IV, the demonstrations are introduced, discussed, and their results presented. Finally, Section V discusses the obtained results and the opportunities for future research. The technical details are diverted to topical appendices: Appendix A contains the proof of an important lemma stated in the theoretical section, Appendix B contains technical details regarding the post-processing steps during the extractions, and Appendix C contains technical details regarding the data analysis of the demonstrations section.

II. NOTATION AND TERMINOLOGY

In this work, two quantum graph states play a central role: we define *linear cluster states* $|L\rangle$ and *GHZ states* $|GHZ\rangle$ as

$$|L\rangle_{\{1,\dots,n\}} := \frac{1}{2^n} \bigotimes_{i=1}^n (|0\rangle + |1\rangle \sigma_z^{i+1})$$

$$|GHZ\rangle_{\{1,\dots,m\}} := \frac{1}{\sqrt{2}} \left(\bigotimes_{i=1}^m |0\rangle + \bigotimes_{i=1}^m |1\rangle \right)$$

and $|L\rangle_V, |GHZ\rangle_V$ as the states corresponding to the vertex set V . When context permits, with e.g. $|L\rangle_n$ we denote the linear cluster state of size n .

Our resource state is the n -partite linear cluster state $|L\rangle_{V_L}$. As a graph state it corresponds to a line graph on the vertices $V_L := \{1, 2, \dots, n\}$. Here, each vertex i corresponds to

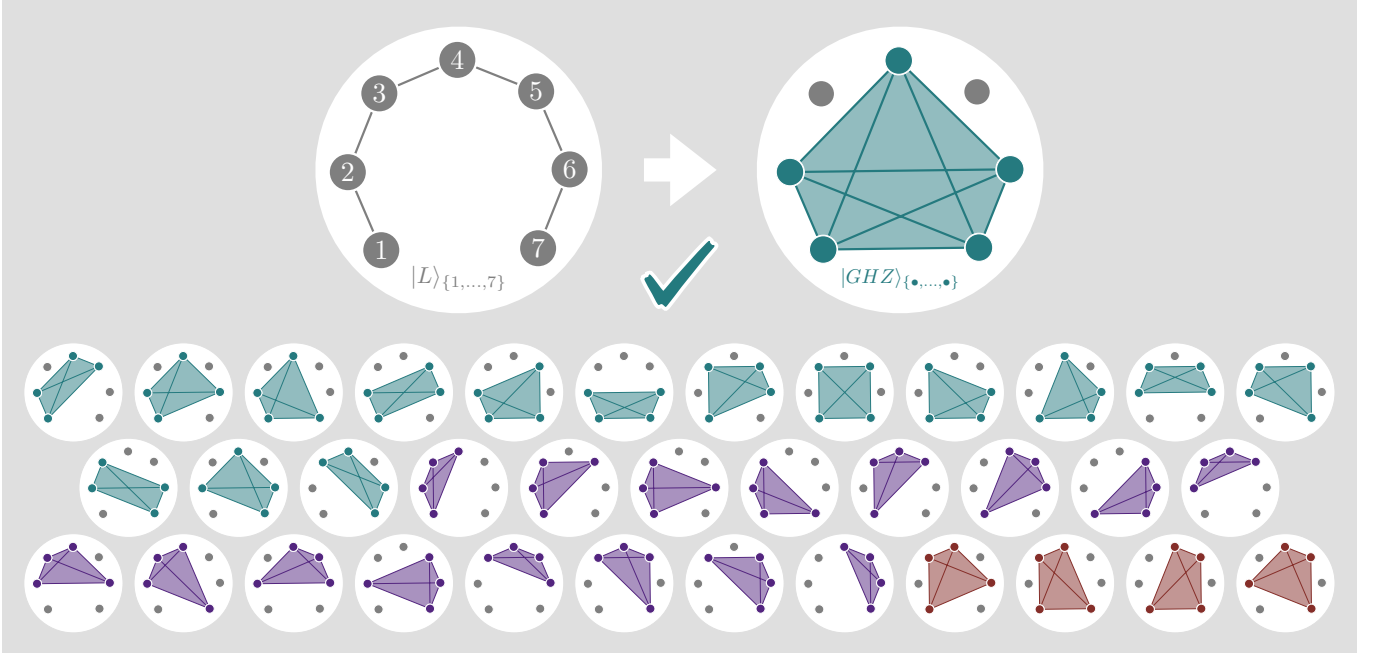


Figure 1: **Example of extracting GHZ states from a linear cluster state with seven qubits:** The only 5-partite GHZ state that can be extracted from this resource is on the qubits corresponding to 1, 2, 4, 6, 7 and is highlighted in green. For 4-partite GHZ states, we also highlight all 15 possible extraction patterns in green, while the patterns in brown are impossible due to Lemma 1 and the patterns shown in violet are impossible due to both Corollary 1 and Lemma 1. Note that due to Theorem 1 it is impossible to extract GHZ states with six or more qubits from this resource – it is however trivially possible to extract all combinations of three-partite GHZ states.

the i -th qubit of $|L\rangle_{V_L}$ and the edges of the graph correspond to nearest-neighbour entangling controlled phase gates. This structure allows us to use the terms *left* and *right* neighbours of i to indicate any vertices h, j with $h < i, i < j$, respectively; e.g. the *direct* left and right neighbours of i are $i \pm 1$.

Let $V_G \subset V_L$ be a set of vertices for which we can extract a GHZ state from the linear cluster resource state. Performing Pauli measurements on the qubits corresponding to $V_M := V_L \setminus V_G$, we obtain a post-measurement state which is local-Clifford equivalent to the $|GHZ\rangle_{V_G}$ state. By performing local operations based on the measurement outcomes, the state can then be locally transformed into this GHZ state.

This construction allows for V_G to inherit the neighbour structure from the linear network V_L : For a vertex $j \in V_G$, we use j_- and j_+ to indicate the left and right neighbour of j in V_G , respectively. We refer to the smallest and largest element of V_G as the *boundaries* of the GHZ state. We finally define any selection of consecutive vertices $i, i+1, \dots, i+k \in V_G$ as a k -*island*.

III. MAIN RESULTS

We now examine what are the different types of GHZ states one can obtain from a given linear cluster state. We first provide an upper bound for the size $|V_G|$ of the extracted GHZ state, and we then show how to saturate it. In order to achieve this, we use Lemma 1, which provides an impossibility result for 2-islands (the proof can be found in App. A).

Lemma 1. *No 2-island can have both a left and a right neighbour in V_G . If two vertices $i, i+1$ are in V_G , then there is*

either no vertex to the left of i or no vertex to the right of $i+1$.

Lemma 1 implies that all vertices i in the target GHZ state must be ‘isolated’ in the linear cluster state; $i-1$ and $i+1$ cannot be in V_G (with the exception of the boundaries). A corollary for 3-islands follows directly:

Corollary 1. *If V_G contains a 3-island, then $|V_G| = 3$.*

Proof. Let $i, i+1, i+2$ be a 3-island in V_G and assume that $|V_G| \geq 4$, i.e. that we have $h < i$ or $j > i+2$ in V_G . This implies that either $i, i+1$ form a 2-island with both left-neighbour h and right-neighbour $i+2$ or $i+1, i+2$ form a 2-island with both left-neighbour i and right-neighbour j . Both are in direct contradiction to Lemma 1. \square

By the same argument, k -islands with $k \geq 4$ are impossible. Ultimately, such k -islands would contain 3-islands in contradiction to Corollary 1. Figure 1 illustrates examples.

This allows us to calculate the upper bound to $|V_G|$.

Theorem 1. *The size of a GHZ state extractable from an n -partite linear cluster state via local Clifford operations, local Pauli measurements, and local unitary corrections, is upper-bounded as $|V_G| \leq \lfloor \frac{n+3}{2} \rfloor$.*

Proof. As there are at most two 2-islands, for every other i in V_G both $i \pm 1$ were measured. Thus, to maximize $|V_G|$, we may have $1, 2, n-1, n$ in V_G , and V_M containing every other vertex in between: For n odd, $V_M = \{3, 5, \dots, n-2\}$; for n even $V_M = \{3, 5, \dots, n-5, n-3, n-2\}$ ¹. In the even case,

¹ In the case of n being even, there is more than one such pattern. While we

$n - 2$ must be measured due to Corollary 1. In both cases $|V_G| = n - |V_M|$ is upper bounded by $\lfloor \frac{n+3}{2} \rfloor$. \square

For example, the largest GHZ state that can be extracted from the 7-qubit linear cluster state shown in Figure 1 is the $|\text{GHZ}\rangle_5$ state where $V_G = \{1, 2, 4, 6, 7\}$ and $V_M = \{3, 5\}$. Figure 1 further shows all possible and impossible selections of V_G to extract the $|\text{GHZ}\rangle_4$ state.

We now show that there is a set of measurements that saturates the bound of Theorem 1 by explicitly giving such a measurement pattern. For $n \leq 5$ this pattern was shown in Ref. [20]. For the general case, let us consider a case distinction with respect to the parity of n :

First, for odd n we can choose $V_M = \{2i+1\}_{i=1}^{\frac{n-3}{2}}$ and every corresponding qubit to be measured in the σ_x -basis; we refer to this measurement pattern as the *maximal* pattern. Below, we show that this pattern actually gets the desired GHZ state.

The linear cluster state is a stabilizer state, i.e. it is an element of the shared $+1$ eigenspace of the operators $\{l_i = \sigma_z^{i-1} \sigma_x^i \sigma_z^{i+1}\}_{i \in V_L}$, where σ_z^0 and σ_z^{n+1} are set equal to the identity. This set of operators forms the set of canonical *generators* of an Abelian subgroup of the n -qubit Pauli group known as the *stabilizer* of the linear cluster states. For an overview of the stabilizer formalism and stabilizer measurements in particular see [23], [24].

Consider the generator transformation

$$l_2 \rightarrow l'_2 = l_2 l_4 \dots l_{n-4} l_{n-2} := \sigma_z^1 \sigma_z^n \prod_{2i \in V_L} \sigma_x^{2i},$$

which ensures that l'_2 and all odd-indexed generators commute with all measurement operators $\{\sigma_x^{j_0}\}_{j_0 \in V_M}$. The post-measurement state is determined by replacing the other $|V_M|$ generators $\{l_{2i}\}_{i=2}^{\frac{n-1}{2}}$ with the measurement operators – together with a multiplicative phase depending on the respective measurement outcome. Then (after removing the support on the measured qubits and applying a Hadamard transformation to 1 and n) the post measurement state on V_G is characterized by the generators $\sigma_x^{V_G}$ and $\{m_{j_0} \sigma_z^{j_0} \sigma_z^{j_0+}\}_{j_0 \in V_G \setminus \{n\}}$, where the $m_{j_0} = \pm 1$ are phases due to the measurement outcomes. These phases can be accounted for by applying σ_x -operations to a selection of the nodes, recovering the generators of the $|\text{GHZ}\rangle_{V_G}$ state. The number of measurements implies $|V_G| = n - |\{3, 5, \dots, n-2\}| = \frac{n+3}{2}$ which saturates the bound for odd n .

Second, for even n it suffices to observe that a σ_z -measurement on the qubit corresponding to n yields a linear cluster state $|L\rangle_{\{1, 2, \dots, n-1\}}$ up to a randomized σ_z^{n-1} -correction depending on the measurement outcome. In analogy to the odd parity case we then obtain $V_M = \{3, 5, \dots, n-3, n\}$ such that $|V_G| = n - |V_M| = \frac{n+2}{2} = \lfloor \frac{n+3}{2} \rfloor$ for even n .

have chosen here to measure the two consecutive vertices, $n-3$ and $n-2$, other possibilities would have been to measure consecutive vertices further to the left and measure only the even vertices to the right. Another option would have been to measure not two consecutive vertices, but a vertex of one of the 2 islands, i.e. either $1, 2, n-1$ or n . It is important to note that all resulting sets V_M have the same size.

Note that the even-case analysis above also applies for measuring an ‘internal’ node in the σ_y -basis, rather than the first or last; this does introduce a Clifford rotation on the two neighbours of the node which needs to be accounted for [25]. The resulting state is then also LOCC equivalent to an $(n-1)$ -partite linear cluster state on the remaining nodes, from which in turn a $|\text{GHZ}\rangle_{\frac{n+2}{2}}$ state can be extracted through the maximal pattern. This approach can be extended to more measurements, where additional ‘inside’ nodes are measured in the σ_y -basis, and ‘outside’ nodes are measured in the σ_z -basis. It is straightforward to see that any choice V_G allowed by Lemma 1 can be seen as arising from such a setting.

Finally, note that while Lemma 1 does allow 2-islands on the boundaries of the extracted GHZ states, they do not necessarily have to be contained in them. For example, $|\text{GHZ}\rangle_{\{1, 3, 5, 7\}}$ can be extracted from $|L\rangle_{\{1, \dots, 7\}}$ as shown in Figure 1. Rigorously stated, this pattern does not arise from one of the maximal patterns defined above, but can instead be considered as a maximal pattern $|\text{GHZ}\rangle_{\{0, 1, 3, 5, 7, 8\}}$ extracted from $|L\rangle_{\{0, \dots, 8\}}$. Here, the additional qubits corresponding to 0 and 8 are just “virtual” and not really there; they simply help visualize all possible patterns: $|\text{GHZ}\rangle_{\{1, 3, 5, 7\}}$ can be extracted from the “virtual” state $|\text{GHZ}\rangle_{0, 1, 3, 5, 7, 8}$ by measuring qubits 0 and 8 in the σ_x -basis. The measurements on the other qubits are unaffected by this; the physical measurements of 2, 4, 6 to obtain $|\text{GHZ}\rangle_{\{1, 3, 5, 7\}}$ from $|L\rangle_{\{1, \dots, 7\}}$ are exactly the same as the ones that would be required to obtain $|\text{GHZ}\rangle_{\{0, 1, 3, 5, 7, 8\}}$ from the “virtual” $|L\rangle_{\{0, \dots, 8\}}$. In this sense, all possible selections of V_G can be seen as subsets of the maximal measurement patterns defined above.

These measurement patterns result in states LOCC equivalent to GHZ states; for explicit calculations of the necessary corrections to obtain the GHZ states themselves we refer to the supplementary material in [25].

IV. DEMONSTRATIONS

We used the IBMQ Montreal device to demonstrate our protocol for the maximal extraction of GHZ states from resource linear cluster states. For odd $n \in \{5, 7, \dots, 19\}$ we prepared the state

$$|\psi\rangle_n = \bigotimes_{i \text{ odd}} H^i |L\rangle_{\{1, \dots, n\}}, \quad (1)$$

i.e. the linear cluster state with every odd qubit rotated to the σ_x -basis. We then extract GHZ states for $m \in \{\frac{n+3}{2}\}_n = \{4, 5, \dots, 11\}$ using the maximal pattern described in the previous section.

Implementing $|\psi\rangle_n$ instead of $|L\rangle_{\{1, \dots, n\}}$ allows us to reduce the circuit depth of the preparation circuit by one, when compiling for the gateset of the IBMQ Montreal device (Pauli-basis rotations, $CNOT$; see Figure 2). When considering the GHZ extraction, this approach has further benefits; the necessary Hadamard transformations on the first and last qubit have, in essence, been applied ‘in advance’, and

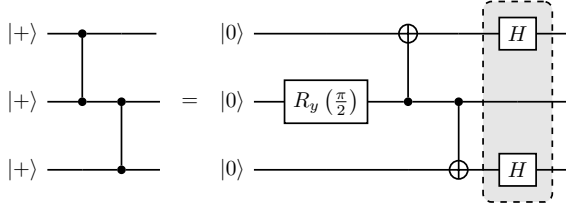


Figure 2: The circuit on the left and on the right are equal; the circuit on the left is the standard preparation of the $|L\rangle_3$ state. The generalization to $|L\rangle_n$ for higher (odd) n follows naturally. The circuit on the right is the compiled version for the IBMQ Montreal chip. By not implementing the single-qubit gates in the grey box, the circuit depth is reduced by 25%. This results in a rotated linear cluster state $|\psi\rangle_n$ as defined in Eq.(1). This state carries the same entanglement properties as the $|L\rangle_n$ state, and most notably can still be used to extract $|GHZ\rangle$ states by adapting the measurement bases.

the σ_x -measurements prescribed by the maximal pattern become σ_z -measurements, which are native to the device. The Pauli-based flips due to the measurement outcomes that are necessary to obtain the GHZ state can be performed in post-processing, as all the subsequent measurements on the GHZ state itself are in the Pauli basis.

To benchmark the results, we compute an estimate for the lower bound of the fidelity for both the linear cluster states and the GHZ states extracted from them. For the linear cluster states we use methods adapted from [26] using insights originally presented in [27]; two measurement settings suffice to estimate the lower bound – one in which all qubits are measured in the σ_z -basis, and one in which all qubits are measured in the σ_x -basis. For the GHZ states we derive a similar technique. Again, two measurement settings suffice – one where all the qubits of the GHZ state are measured in the σ_z -basis, and one where all the qubits of the GHZ are measured in the σ_x -basis. Both these measurement settings are performed in parallel to the σ_z -measurements of the qubits not included in the GHZ state that are required for the extraction. All measurements are repeated 32000 times to calculate estimates for the expectation values.

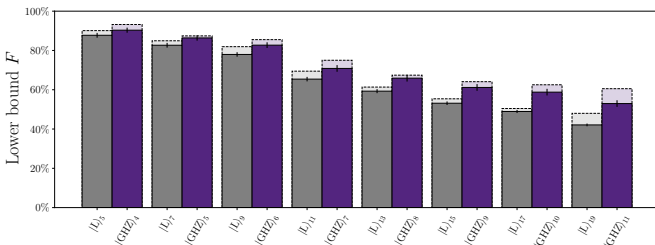


Figure 3: A lower bound of the fidelity of the rotated linear cluster and GHZ states prepared on the IBMQ Montreal device. We prepared rotated (see Eq. 1) linear cluster states $|\psi\rangle_n$ for $n \in \{5, 7, \dots, 19\}$ and extracted $|GHZ\rangle_m$ states for $m \in \{4, 5, \dots, 11\}$ using the maximal pattern introduced in Sec. III. For states with a higher number of qubits, the lower bound on the linear cluster state is increasingly worse due to a technical aspect of the estimation method (see App. C for details). The results are ordered such that each linear cluster state $|L\rangle_n$ is paired with the $|GHZ\rangle_m$ state extracted from it.

Figure 3 shows the lower bounds on the fidelity for all linear cluster states that we generated with the IBMQ Montreal device – as well as for the GHZ states we extracted from them. Note that our estimation method imposes a relative penalty for linear cluster state fidelity estimations compared to GHZ

state fidelity estimations. However, this does not mean that the fidelity of the GHZ states is truly higher than that of the linear cluster states from which they were extracted: It simply means that we have used a method of bounding the fidelity from below, which works comparatively better for GHZ states than it does for linear cluster states. For the details of the estimation method we refer to App. C.

V. DISCUSSION

In this letter, we considered how to establish GHZ states between nodes that are share entanglement only with only a small number of nearest neighbours. In particular, given a linear cluster state shared between the nodes, we showed what are the possible GHZ states that can be obtained, the later being an indispensable resource in many quantum communication protocols including secret sharing [16], electronic voting [28] and anonymous conference key agreement [18].

Our results demonstrate that this process is possible but costly, since almost half of the linear cluster state qubits must be measured to obtain a GHZ state on the remaining qubits. Very importantly, we showed that there is in fact a tight upper bound to the size of the GHZ state we can obtain, higher than the one previously conjectured [7], thus solving a long-lasting open problem. We finally gave an exhaustive characterization of all possible GHZ states that can be extracted and provided a constructive method to obtain them, including the calculations for the necessary local rotations on the remaining qubits.

Our theoretical results are complemented by an implementation on IBM's superconducting quantum hardware, where this near-neighbour architecture is inherent. With fidelities of 80% and higher for up to nine qubits, the results show that the generation of multi-partite entangled states is possible. It is also evident from the shown results that our method of extracting GHZ states does not compromise the fidelity of the target states compared to the resource states, since only local operations are required. Since the generation of linear cluster states can be, depending on the specific setting, experimentally more feasible, our approach shows a potentially more robust method of generating GHZ states.

Finally, extending our methods to other simple graph state resources does not seem trivial and requires further research. We note, however, that deriving an analogous characterisation for ring graph states, i.e. graph states in which the leftmost and rightmost qubits of an otherwise linear cluster state are also connected, is straightforward using our methods. In this case, only a single 2-island is possible, so the upper bound for $|V_G|$ becomes $\lfloor \frac{n+1}{2} \rfloor$.

VI. ACKNOWLEDGEMENTS

A.P., J.d.J. and F.H. acknowledge support from the German Research Foundation (DFG, Emmy Noether Grant No. 418294583) and from the European Union via the Quantum Internet Alliance project. Upon completion of this work, we became aware of work similarly motivated [21, 22].

- [1] D. M. Greenberger, M. A. Horne, and A. Zeilinger, “Going beyond bell’s theorem,” in *Bell’s Theorem, Quantum Theory and Conceptions of the Universe*, edited by M. Kafatos (Springer Netherlands, Dordrecht, 1989) pp. 69–72.
- [2] M. Hein, W. Dür, J. Eisert, R. Raussendorf, M. V. d. Nest, and H.-J. Briegel, *Entanglement in Graph States and its Applications*, Tech. Rep. arXiv:quant-ph/0602096 (arXiv, 2006) arXiv:quant-ph/0602096 type: article.
- [3] D.-M. Schlingemann, *Journal of Mathematical Physics* **45**, 4322 (2004).
- [4] M. Hein, J. Eisert, and H. J. Briegel, *Physical Review A* **69**, 062311 (2004).
- [5] A. Bouchet, *Journal of Combinatorial Theory, Series B* **45**, 58 (1988).
- [6] F. Hahn, A. Dahlberg, J. Eisert, and A. Pappa, *Phys. Rev. A* **106**, L010401 (2022).
- [7] H. J. Briegel and R. Raussendorf, *Physical Review Letters* **86**, 910 (2001).
- [8] M. Van den Nest, J. Dehaene, and B. De Moor, *Physical Review A* **69**, 022316 (2004).
- [9] M. Van den Nest, J. Dehaene, and B. De Moor, *Physical Review A* **71**, 062323 (2005).
- [10] A. Dahlberg and S. Wehner, *Philosophical Transactions of the Royal Society A: Mathematical, Physical and Engineering Sciences* **376**, 20170325 (2018).
- [11] A. Dahlberg, J. Helsen, and S. Wehner, *Quantum Science and Technology* **5**, 045016 (2020).
- [12] A. Dahlberg, J. Helsen, and S. Wehner, *Journal of Mathematical Physics* **61**, 022202 (2020).
- [13] A. Dahlberg, J. Helsen, and S. Wehner, *Quantum* **4**, 348 (2020).
- [14] M. Christandl and S. Wehner, in *Advances in Cryptology - ASIACRYPT 2005*, Vol. 3788, edited by D. Hutchison, T. Kanade, J. Kittler, J. M. Kleinberg, F. Mattern, J. C. Mitchell, M. Naor, O. Nierstrasz, C. Pandu Rangan, B. Steffen, M. Sudan, D. Terzopoulos, D. Tygar, M. Y. Vardi, G. Weikum, and B. Roy (Springer Berlin Heidelberg, Berlin, Heidelberg, 2005) pp. 217–235, series Title: Lecture Notes in Computer Science.
- [15] M. Hillery, V. Bužek, and A. Berthiaume, *Phys. Rev. A* **59**, 1829 (1999).
- [16] A. Broadbent, P.-R. Chouha, and A. Tapp, in *2009 Third International Conference on Quantum, Nano and Micro Technologies* (2009) pp. 59–62.
- [17] G. Murta, F. Grasselli, H. Kampermann, and D. Bruß, *Advanced Quantum Technologies* **3**, 2000025 (2020), eprint: <https://onlinelibrary.wiley.com/doi/pdf/10.1002/qute.202000025>.
- [18] F. Hahn, J. de Jong, and A. Pappa, *PRX Quantum* **1**, 020325 (2020).
- [19] F. Grasselli, G. Murta, J. de Jong, F. Hahn, D. Bruß, H. Kampermann, and A. Pappa, *PRX Quantum* **3**, 040306 (2022).
- [20] F. Hahn, A. Pappa, and J. Eisert, *npj Quantum Information* **5**, 76 (2019).
- [21] R. Frantzeskakis, C. Liu, Z. Raissi, E. Barnes, and S. E. Economou, arXiv preprint arXiv:2203.07210 (2022).
- [22] V. Mannalath and A. Pathak, “Multiparty Entanglement Routing in Quantum Networks,” (2022), arXiv:2211.06690 [math-ph, physics:quant-ph].
- [23] D. Gottesman, “Stabilizer codes and quantum error correction,” (1997).
- [24] D. Gottesman, “The Heisenberg representation of quantum computers,” (1998).
- [25] “Supplementary information to the paper “Extracting maximal entanglement from linear cluster states”,” <https://github.com/hahnfrederik/Extracting-maximal-entanglement-from-linear-cluster-states> (2022), [Online; accessed 25-November-2022].
- [26] K. Tiurev and A. S. Sørensen, *Phys. Rev. Research* **4**, 033162 (2022).
- [27] G. Tóth and O. Gühne, *Phys. Rev. Lett.* **94**, 060501 (2005).
- [28] P. Xue and X. Zhang, *Scientific Reports* **7**, 7586 (2017).
- [29] J. Dehaene and B. De Moor, *Phys. Rev. A* **68**, 042318 (2003).

Appendix A: Proof of Lemma 1

In this section we proof Lemma 1. We prove the theorem by contradiction. Fix a set V_G such that $\{i, i+1\} \subset V_G$ and let the post-measurement state $|\psi\rangle_{V_G}$ be locally equivalent to $|\text{GHZ}\rangle_{V_G}$. Assume now that there are both $j < i$ and $k > i+1$ for which both $j, k \in V_G$. W.l.o.g. assume that j and k are the direct left- and right neighbour of i and $i+1$, respectively.

Recall that a set of generators for the linear cluster state is $\{l_{i_0} = \sigma_z^{i_0} \sigma_x^{i_0} \sigma_z^{i_0+1}\}_{i_0 \in V_L}$. If the post-measurement state is locally equivalent to the GHZ state then there must exist a (reversible) generator transformation such that their support on i and $i+1$ coincides exactly with (the generators of) the GHZ state - up to local Clifford rotations. We will now show that, from a reversible transformation of the $\{l_{i_0}\}$, it is impossible to obtain such a set of generators when $j, i, i+1, k \in V_G$. This directly implies that a measurement pattern such that the GHZ state can be obtained is not possible.

(A set of) generators for the GHZ state are, $\{\sigma_x^{V_G}\} \cup \{\sigma_z^{i_0} \sigma_z^{i_0+1}\}_{i_0 \in V_G}$, where it is implied that $\sigma_z^{i_0+1} = 1$ when $i_0 \notin V_G$. Focusing on i and $i+1$, the only generators with non-trivial support are $\{\alpha, \beta, \gamma, \delta\} = \{\sigma_{a_i}^i, \sigma_{a_i}^i \sigma_{a_{i+1}}^{i+1}, \sigma_{a_{i+1}}^{i+1}, \sigma_{b_i}^i \sigma_{b_{i+1}}^{i+1}\}$, where $a_i, a_{i+1}, b_i, b_{i+1} \in \{x, y, z\}$ reflect the fact that the state is *locally equivalent* to the GHZ state. This implies that $a_i \neq b_i$ and $a_{i+1} \neq b_{i+1}$.

Similarly, only the generators l_{i-1}, l_i, l_{i+1} and l_{i+2} of the linear cluster state (i.e. those with support on i or $i+1$) can have a non-trivial contribution to the generator transformation on the vertices in question. Therefore, w.l.o.g., we can focus on just these four generators and restrict our attention to vertices i and $i+1$. If we show that there is no reversible transformation of $\{l_k\}_{k=\{i-1, i, i+1, i+2\}}$ to obtain $\{\alpha, \beta, \gamma, \delta\}$ when only considering these nodes, the lemma follows. We show there is no such transformation by exhaustive contradiction.

There are three different ways of creating generator α : **i)** $\alpha \propto l_{i-1} = \sigma_z^i$, **ii)** $\alpha \propto l_i \circ l_{i+2} = \sigma_x^i$, **iii)** $\alpha \propto l_{i-1} \circ l_i \circ l_{i+2} = \sigma_y^i$, where ‘ $\alpha \propto l_{i-1}$ ’ should be read as ‘ l_{i-1} takes the role of α ’, and \circ denotes the (qubit-wise) product (e.g. $l_i \circ l_{i+1} = \sigma_x^i \sigma_z^{i+1} \circ \sigma_z^i \sigma_x^{i+1} \triangleq \sigma_y^i \sigma_y^{i+1}$, where the last equality is up to an irrelevant global phase). Similarly, there are three different ways of creating generator γ : **j)** $\gamma \propto l_{i+2} = \sigma + z^{i+2}$, **jj)** $\gamma \propto l_{i-1} \circ l_{i+1} = \sigma_x^{i+2}$, **jjj)** $\gamma \propto l_{i-1} \circ l_{i+1} \circ l_{i+2} = \sigma_y^{i+2}$. Picking e.g. **i)** and **j)** one sees that β is fixed at

$\propto \sigma_z^i \sigma_z^{i+1}$. But this is $l_{i-1} \circ l_{i+2} \propto \alpha \circ \gamma$, which would not be a reversible transformation of the generators l_{i-1}, l_i, l_{i+1} and l_{i+2} . Any other pair from $\{\mathbf{i}, \mathbf{ii}, \mathbf{iii}\}$ and $\{\mathbf{j}, \mathbf{jj}, \mathbf{jjj}\}$ would also necessitate such a non-reversible transformation.

In essence, when viewing the generators as vectors over \mathbf{F}_2^{2n} through the binary representation [29], the argument follows from the observation that (the vector associated with) β lies in the subspace spanned by (the vectors associated with) α and γ . As such there can never be a reversible (i.e. basis-preserving) operation on (the vectors associated with) l_{i-1}, l_i, l_{i+1} and l_{i+2} that obtains α, β and γ .

Appendix B: Local-Clifford corrections to obtain GHZ states.

We provide a jupyter notebook for determining the required correction operations under [25].

Appendix C: Estimation of lower bound for fidelity in the demonstrations.

We here provide details for the method of estimation of the lower bound of the fidelity of both the linear cluster state and GHZ state, that has been used in the demonstrational implementation. The method is presented in and adapted from [26] using insights originally presented in [27]. The state that is prepared is

$$|\psi\rangle_n = \bigotimes_{i \text{ odd}} H^i |L\rangle_n,$$

which is a linear cluster state rotated by Clifford operations and thus a stabilizer state. Note that the generators G^L for the stabilizer of $|\psi\rangle_n$ can be grouped into ‘odd’ generators $G_o^L = \{\sigma_z^{i-1} \sigma_z^i \sigma_z^{i+1}\}_{i \text{ odd}}$ and ‘even’ generators $G_e^L = \{\sigma_x^{i-1} \sigma_x^i \sigma_x^{i+1}\}_{i \text{ even}}$, where again $\sigma_z^0 = \sigma_z^{n+1} = 1$. The fidelity of the prepared state ρ with the rotated linear cluster state is $F(\rho, |\psi\rangle_n) = \text{tr}[\rho |\psi\rangle\langle\psi|_n]$. Writing $G_{o(e)} = \prod_{g \in G_{o(e)}^L} \frac{\mathbb{I} + g}{2}$, and using $|\psi\rangle\langle\psi|_n = \prod_{g \in G} \frac{\mathbb{I} + g}{2} = G_o G_e$, we can write

$$\begin{aligned} F(\rho, |\psi\rangle_n) &= \text{tr}[G_o G_e \rho] \\ &= \text{tr}[G_o \rho] + \text{tr}[G_e \rho] - \text{tr}[\mathbb{I} \rho] + \text{tr}[K \rho], \end{aligned}$$

where $K = (\mathbb{I} - G_o)(\mathbb{I} - G_e)$. K is positive semidefinite and thus we can discard the last term to obtain a lower bound

for the fidelity:

$$F(\rho, |\psi\rangle_n) \geq \mathbb{E}[G_o] + \mathbb{E}[G_e] - 1,$$

where $\mathbb{E}[G_{o(e)}] = \frac{1}{2^{|S_{o(e)}|}} \sum_{\sigma \in S_{o(e)}} \text{tr}[\rho \sigma]$ with $S_{o(e)} = \langle G_{o(e)}^L \rangle \subset \mathcal{S}$ the subgroup generated by the ‘odd’ (‘even’) generators of $|\psi\rangle_n$. Notably, all terms $\text{tr}[\rho \sigma]$ comprise of only σ_z -basis ($\sigma \in \mathcal{S}_o$) or σ_x -basis ($\sigma \in \mathcal{S}_e$) measurements. This means that just two measurement settings suffice to estimate the lower bound: measuring all vertices in the σ_z -basis, and measuring all vertices in the σ_x -basis. By repeating these measurements 32000 times and obtaining the outcome statistics, we estimate all terms $\text{tr}[\rho \sigma]$ by selecting the outcomes associated with the +1 and -1 eigenspaces of all different observables.

For the GHZ state we use a similar method, where we now group the generators G^G of the GHZ state into $G_o^G = \{\sigma_x^{V_G}\}$ and $G_e^G = \{\sigma_z^j \sigma_z^{j+}\}_{j \in V_G}$, which again allows for an estimate of the lower bound with just two measurement settings. A caveat is that now there is only one ‘odd’ generator and thus $\mathbb{E}[G_o^G] = \frac{1}{2} \text{tr}[\rho \mathbb{I}] + \frac{1}{2} \text{tr}[\rho \sigma_x^{V_G}]$. By definition $\text{tr}[\rho \mathbb{I}] = 1$ and therefore the expectation value is more skewed towards 1 than for the linear cluster state estimation. In other words it gives a higher bound on the fidelity when compared to the linear cluster state, since $G_o^L = O(2^n)$ and as such the identity does not have such a strong impact on the estimate, especially for larger linear cluster states. To give another comparison between the two states, Figure 4 contains the same results as Figure 3 from the main text, but with the identity-term omitted. This gives a lower but more equal estimate for both classes of states.

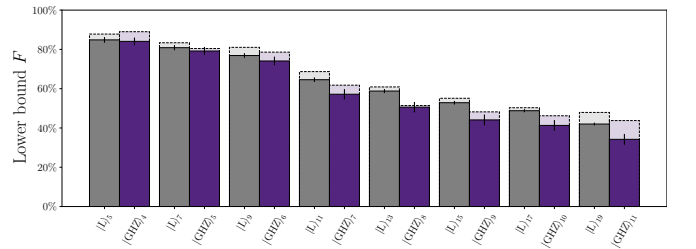


Figure 4: Lower bound on the fidelity using an adapted estimate method. In comparison with Figure 3, positive terms that favour the GHZ states are dropped, which renders a lower but more equal estimate on the fidelities for all states.